Journal of Applied Sciences

ISSN 1812-5654

science alert

ANSInet
an open access publisher
http://ansinet.com

Journal of Applied Sciences 11 (10): 1733-1740, 2011
ISSN 1812-5654 / DOI: 10.3923/jas.2011.1733.1740

Analysis of the Temperature Distribution in GT Blade Cooled by Compressed Air

Hussain H. Al-Kayiem and Amir H. Ghanizadeh
Department of Mechanical Engineering, Universiti Teknologi PETRONAS,
Bandar Seri Iskandar, 31750, Tronoh, Perak, Malaysia

Abstract: As the gas turbine inlet temperature increases, the heat transferred to the turbine blade also increases. The operating temperatures are far above the permissible metal temperatures. Therefore, there is a critical need to cool the blades for safe operation. In the present study the internal cooling of a gas turbine blade is analyzed. The blade has a rectangular 9×18 mm compressed air channel along the blade span. Finite-Difference method is used to predict temperature distribution for blade cross section at different heights from the root. Effect of compressed air mass flow rate, inlet temperature and the temperature of combustion gasses have been considered. The investigations are carried out for both smooth and two opposite ribbed-walls channels. The results are presented and discussed as temperature distribution in various sections of the blade and also the comparison between ribbed and smooth channel hydrothermal values. Various ribs configurations have been considered in the analysis. Results at rib angles, α of 90, 60, 45 and 30° and ribs blockage ratios, e/D_h ranging from 0.042 to 0.078 are compared in terms of Nu and friction factor, f. It is found that maximum Nu number occurs when 60° ribs are introduced in the channel. An enhancement of 149.45% is achieved with penalty of increase in the friction factor by 114.5%.

Key words: Gas turbine blade, heat transfer enhancement, numerical analysis, ribbed channel, blade cooling

INTRODUCTION

Gas turbine engines are designed to continuously and efficiently convert the energy of fuel into useful power and are developed into very reliable, high performance engines (high ratio of power output to weight, high efficiency and low maintenance costs). Gas turbines are now widely used in power plants, marine industries and aircraft propulsion.

Over the past fifty years, aircraft and power generation gas turbine designers tried to increase the combustion chamber exit and high-pressure turbine stage inlet temperatures. With higher combustion chamber exit temperatures, improved efficiency and reduced fuel consumption can be achieved. Similarly, in aircraft application, the higher temperatures lead to increased thrust. Unfortunately, these higher temperatures have a negative effect on the integrity of the high-pressure turbine components and specifically the turbine blades (Altorairi, 2003).

High turbine inlet temperatures provide a challenging environment for turbine blades which are subject to a variety of damage mechanisms, including high-temperature oxidation, creep, corrosion and thermo-mechanical fatigue. Therefore, there is a critical need to cool the blades. In internal cooling, air is bled from the compressor stage and then passed through internal passages incorporated into the blade for this purpose (Fig. 1 shows typical coolant channels in turbine airfoil). This extraction incurs a penalty on the thermal efficiency and power output of the engine so it is important to understand and optimize the cooling technology for a given turbine blade geometry under engine operating conditions (Han, 2004).

The objective of the recent study is to present and discuss the temperature distribution results in the GT blade by two cooling methods using compressed air. The temperature distribution in the blade body is estimated in two different cooling channel configurations. In the first type, the channel wall is non-ribbed, or so called smooth. In the second type, regular repeated ribs artificially roughen the channel walls.

MATERIALS AND METHODS

An out of use GT blade has been selected for the recent work. Laser digitizer has identified the blade profile and geometries. It is 21 cm high and having rectangular compressed air passage channel in the leading edge. The air channel has dimensions of a = 9×b = 18 mm.

The cross section is modeled and meshed around the rectangular channel as shown in Fig. 2. Meshing has

Corresponding Author: Hussain H. Al-Kayiem, Department of Mechanical Engineering, Universiti Teknologi PETRONAS, Bandar Seri Iskandar, 31750, Tronoh, Perak, Malaysia

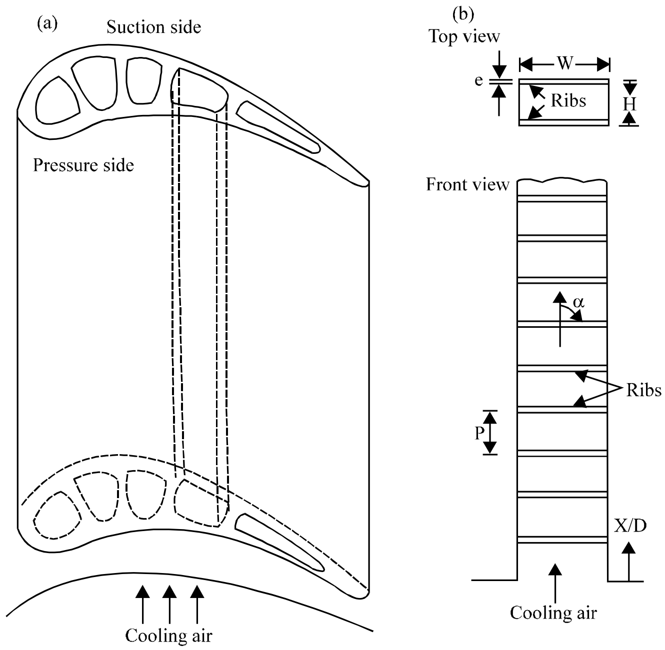

Fig. 1: Typical coolant channels in turbine airfoils and internal rib arrangement (Han *et al*., 2001)

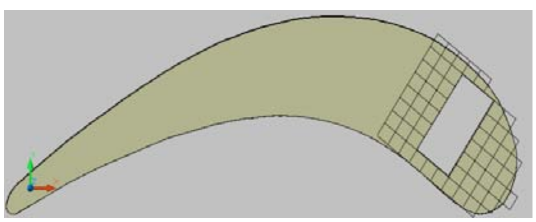

Fig. 2: Cross-section of the modeled GT blade and correspondence meshing around the internal air channel

resulted in 82 nodes. Finite-Difference method is used to find the temperature distribution at the leading edge by solving the set of the nodal equations.

Summary of nodal finite difference equations using square grids are as following:

Interior node:

$$T_{m,n+1}+T_{m,n-1}+T_{m-1,n}+T_{m+1,n}-4T_{m,n}=0 \tag{1}$$

Node at an internal corner with convection:

$$2\,(T_{m-1,n}+T_{m,n+1})+(T_{m,n-1}+T_{m+1,n})+2\frac{h\Delta x}{k}T_\infty -2\,(3+\frac{h\Delta x}{k})T_{m,n}=0 \tag{2}$$

Node at a plane surface with convection:

$$(2T_{m-1,n}+T_{m,n+1}+T_{m,n-1})+2\frac{h\Delta x}{k}T_\infty -2\,(\frac{h\Delta x}{k}+2)T_{m,n}=0 \tag{3}$$

Node at an External corner with convection:

$$(2T_{m-1,n}+T_{m,n+1}+T_{m,n-1})+2\frac{h\Delta x}{k}T_\infty -2\,(\frac{h\Delta x}{k}+2)T_{m,n}=0 \tag{4}$$

Node at a plane surface with uniform heat flux:

$$(2T_{m-1,n}+T_{m,n+1}+T_{m,n-1})+2\frac{q''\Delta x}{k}T_\infty -4T_{m,n}=0 \tag{5}$$

where, k, T_∞, Δx and h are thermal conductivity of the blade, temperature of hot gasses attacking the blade, grid space (Δx = 3 mm) and heat transfer convection coefficient (either for hot gasses or compressed air), respectively.

Considering a typical gas turbine, the following conditions were used (Incropera, 2007):

- Temperature of hot gases attacking the blade is 1700 K
- Temperature of compressed air (T_a) entering the blade root is 400 K

- Convection heat transfer coefficient (h_∞) for the hot gases is 1000 W m^{-2}K
- Mass flow rate of compressed air entering the channel is 0.01 kg sec^{-1}
- Thermal conductivity of the blade is assumed to be 25 W m^{-1}K

Due to the existence of other cooling channels in the blade at left side of the channel in Fig. 2 where the meshing is terminated, an adiabatic line is assumed to exist for these nodes.

Cooling by non-ribbed channels: For a smooth rectangular channel, Reynolds number can be evaluated using hydraulic diameter, D_h:

$$Re_{D_h} = \frac{u_m \rho D_h}{\mu} \quad (6)$$

$$D_h = \frac{4A_c}{P} \quad (7)$$

$$P = 2(a+b) \quad (8)$$

where, ρ, μ, μ_m, A_c and P are density, kinetic viscosity, compressed air velocity, flow cross section area and the wetted parameter, respectively.

Considering $u_m = \dot{m} / (\rho A_c)$ ($\dot{m}$ being air mass flow rate) then:

$$Re_{D_h} = \frac{4\dot{m}}{P\mu} \quad (9)$$

For a turbulent flow, that is fully developed, Nu number can be calculated using Dittus boelter equation with n = 0.4 for heating (Incropera, 2007):

$$Nu = 0.023 Re_D^{4/5} Pr^n \quad (10)$$

Heat transfer convection coefficient and Nu number are related by the following formula:

$$h = \frac{Nu \cdot k}{D_h} \quad (11)$$

COOLING BY RIBBED CHANNELS

In advanced gas turbine blades, repeated rib turbulence promoters are cast on two opposite walls of internal cooling passages to enhance heat transfer. Thermal energy conducts from the external pressure and suction surfaces of the turbine blades into the inner zones and the heat is extracted by internal cooling (Altorairi, 2003). Ribs mostly disturb only the near wall flow and consequently the pressure drop penalty by ribs is acceptable for blade cooling design. There have been many studies to understand heat transfer and flow separation caused by ribs, e.g. (Han, 1988; Han *et al*., 2001; Webb *et al*., 1971).

Findings showed that pressure drop and also the heat transfer is strongly connected to the size of the rib, e and distance between two successive ribs, the pitch, P. In experiments on rib-roughened rectangular channels, most significant parameters, apart from the Reynolds number, Re, are rib blockage ratio e/D_h (D_h is hydraulic diameter of the channel), channel aspect ratio W/H (where W is the width of the ribbed side of the channel and H is the height of the smoothed side and rib angle α.

Han (1988) developed a correlation to predict the performance of two-sided orthogonal ribbed rectangular channels. The roughness function R is given by:

$$R(e^+) = (\frac{2}{f})^{1/2} + 2.5 \ln (\frac{2e}{D} \frac{2W}{W+H}) + 2.5 \quad (12)$$

The roughness Reynolds number e^+ is given by:

$$e^+ = (e/D) Re (f/2)^{1/2} \quad (13)$$

And the heat transfer roughness function G was given by:

$$G(e^+, 0Pr) = R(e^+) + \frac{(f/2St_r) - 1}{(f/2)^{1/2}} \quad (14)$$

The four-sided ribbed channel friction factor f is given by:

$$f = \bar{f} + (H/W)(\bar{f} - f_s) \quad (15)$$

- $\bar{f}$ is average friction factor in a channel with two opposite ribbed walls
- f_s the friction factor for smooth-sided channels

St_r is ribbed sidewall centerline average Stanton number for flow in a channel with two opposite ribbed walls and is related to Nu and h as following:

$$St_r = \frac{Nu}{RePr} = \frac{h}{\rho V C_p} \quad (16)$$

Han *et al*. (1989) obtained the relation between G and e^+ as well as R and α in narrow-aspect ratio rectangular ribbed channels as indicated in the Fig. 4. Therefore, $\bar{f}$ and St_r, for a desired operating condition (given W/H, e/D and Re) can be predicted from experimentally obtained R and G correlations.

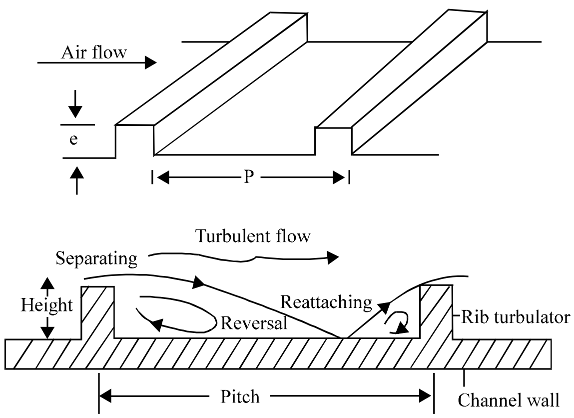

Fig. 3: Schematic of flow separation and rib orientations in heat transfer coefficient enhancement (Han and Dutta, 1995)

Air properties at 400 K are obtained as $\mu = 230.1\times10^{-7}$ Ns m^{-2}, $k_{air} = 33.8\times10^{-3}$W m^{-1}K and Pr ~ 0.7, using (7) to (11) we have Re_D= 32192, Nu = 79.60 and h_{air} = 224.22 W m^{-1}K (Fig. 3).

Having h_{air} for smooth channel (1) to (5) are assigned to appropriate nodes as stated and then solved for temperature distribution around the cooling channel at the root of the blade.

Air temperature continuously changes when flowing inside the channel this in turn changes temperature distribution for every cross section one may choose along the height. Therefore if the height of the blade is segmented, the same procedure can be applied to each segment to find temperature distribution.

It should be noted that h_a and air properties are changing since air temperature entering each segment will differ. This change can be found by calculating the rate of heat transfer (q') per unit length of the channel for each segment as follow (look at Fig. 5 for location of nodes):

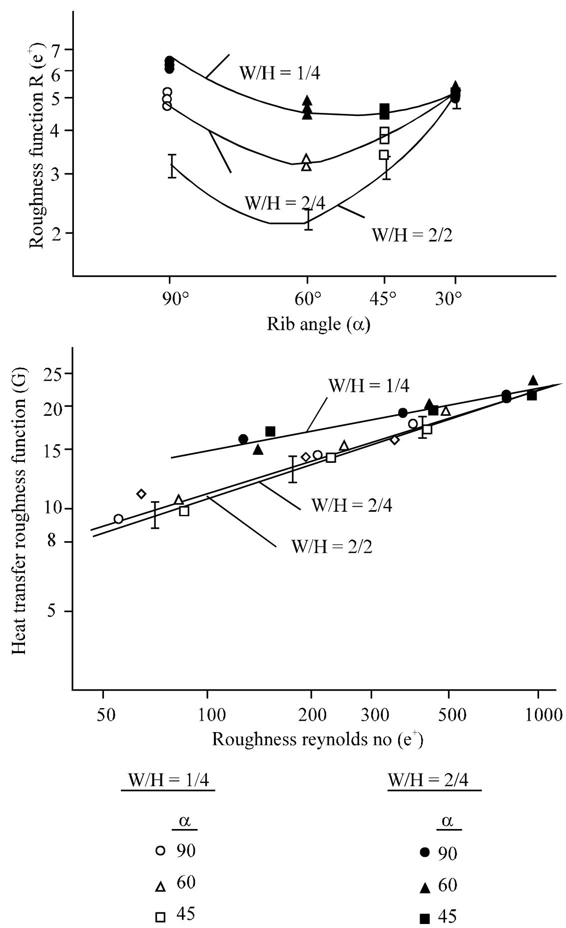

Fig. 4: Friction factor and heat transfer correlation in narrow-aspect ratio rectangular ribbed channels (Han and Dutta, 1995)

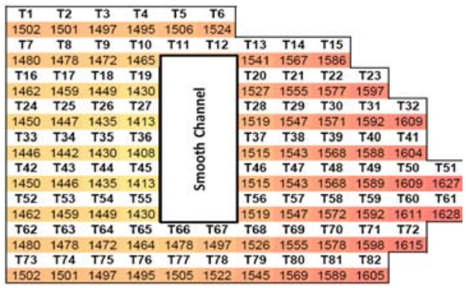

Fig. 5: Temperature (K) distribution in the cross section of GT blade surrounding the cooling passage at root

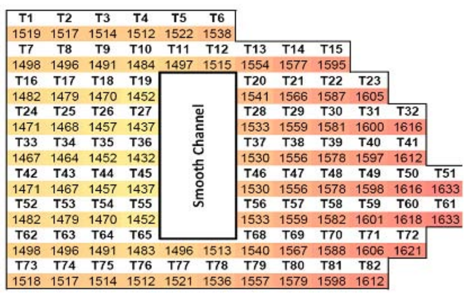

Fig. 6: Temperature (K) distribution in the cross section of the fourth segment (H=15.75 to 21 cm) of GT blade surrounding the cooling passage

$$q' = h_{segment} [\Delta x (T_{20} + T_{28} + T_{31} + T_{46} + T_{56} + T_{19} + T_{27} + T_{36} + T_{45} + T_{55} + T_{10} + T_{11} + T_{65} + T_{68} + T_{66} + T_{67} - 16 \times T_a) + \frac{\Delta x}{2} (T_{12} + T_{13} - 2T_a) + \Delta x (T_\infty - T_a)] \quad (17)$$

Once q' is found and then change in air temperature (ΔT_a) can be calculated easily using:

$$q' \cdot H_{segment} = C_P \cdot \dot{m}_{air} \cdot \Delta T_a \quad (18)$$

where, $H_{segment}$ is height of the segment and C_p is specific heat capacity of air.

If the blade is divided to four equal segments along the height, the temperature distribution at the root segment and at the top segment will be as in Fig. 5 and 6.

Air finally leaves the channel at 659.1 K. If we neglect the changes in air properties when passing throw the channel then air leaves at 673 K, so assuming constant properties of air the error is less than 2%.

RESULTS AND DISCUSSION

Results for smooth channel: Figure 7 shows exit air temperature versus air mass flow rate assuming constant properties, by increasing air mass flow rate; the outlet temperature will decrease and tends to approach inlet temperature. Figure 8 demonstrates air mass flow rate and convection coefficient relation.

According to the results shown in Fig. 9, local convection coefficient increases as air travels to the end

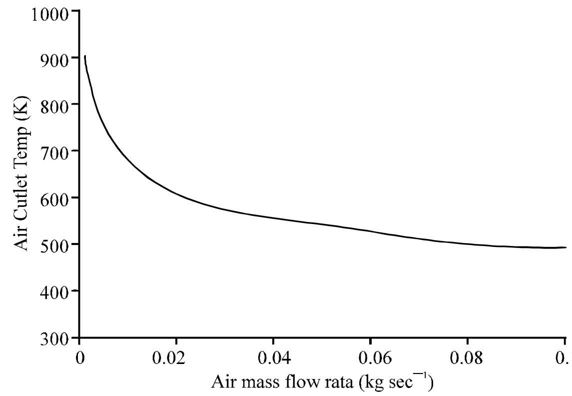

Fig. 7: Air outlet temperature (K) for different mass flow rates (kg sec^{-1}) for smooth channel

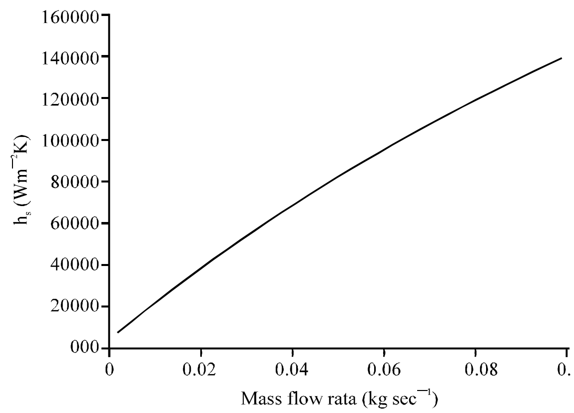

Fig. 8: Convection coefficient (W m^{-2}K) for different air mass flow rates (kg sec^{-1}) in smooth channel

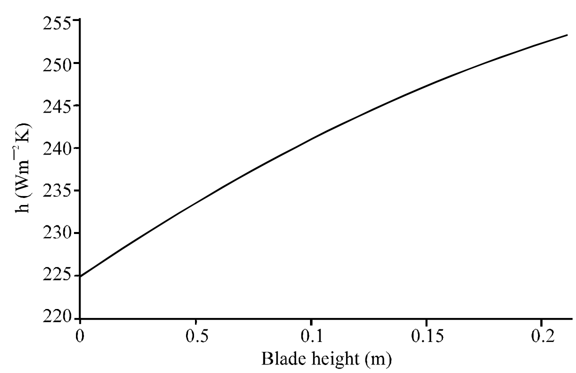

Fig. 9: Local convection coefficient in smooth channel

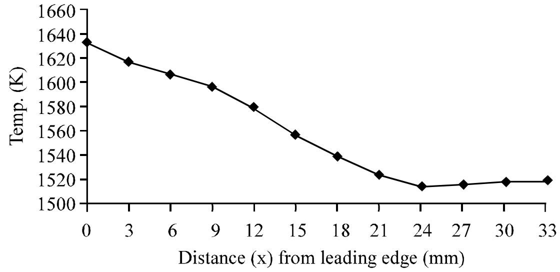

Fig. 10: Temperature (K) distribution along suction surface (H = 15.75 to 21 cm)

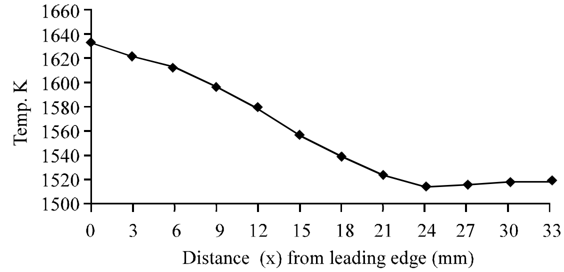

Fig. 11: Temperature (K) distribution along pressure surface (H = 15.75 to 21 cm)

Table 1: Comparison between cooling effect by different k and h_a

$k (W\ m^{-1}K)$	$h_a\ (W\ m^{-2}K)$	T_{max} (K)	$q'\ (W\ m^{-1})$
25	200	1635	11977
50	200	1616	12244
25	400	1585	20972
50	400	1549	21775

of channel. Figure 10 and 11 show temperature distribution along suction and pressure surfaces for the last segment respectively, maximum temperature occurs at the tip.

In the gas turbine industry there is great interest in adopting measures that reduce blade temperatures. Among them is the use of a different alloy of larger thermal conductivity or increasing mass flow rate of coolant through the channel, means increasing h_a. Table 1 shows a parametric variations of k and h_a. It can be concluded that increasing k and h_a reduces temperature in blade but effect of changes in h_a is far more significant than that of k.

Results for ribbed channel: Effect of introducing rib angles, α of 90, 60, 45 and 30° and ribs blockage ratios (e/D_h) ranging from 0.042 to 0.078 to pressure and suction walls of the same channel discussed later are presented here.

Referring to Fig. 4 for this case (W/H =1/2), for orthogonal rib (α = 90°) an approximate value of 5 can be obtained for R. Substituting R = 5, Re = 32192.12 in (12) and assuming rib blockage ratio of e/D_h = 0.063, friction factor for four-sided ribbed channel is calculated as: f = 0.0265. Using (13), e^+ = 233.32, now having value of e^+, G can be evaluated using Fig. 4. However an alternative solution is to use a relation presented by (8) for Pr = 0.7 as follow:

$$G = C\,(e^+)^n \qquad (19)$$

where, n = 0.35 and C = 2.24 if α = 90°. Using (19), G = 15.10. According to (14), St_r = 0.0062 substituting this in (5), heat transfer convection coefficient in the orthogonal ribbed channel with e/D_h = 0.063 is found as h_{ribbed} = 388.53 W m^{-2}K.

Table 2: Friction factor and convection coefficient for ribbed channel at = 0.01 kg sec^{-1}

Rib angle (α)	$R(e^+)$	e/D	$\bar{f}$	$H_{ribbed}\ (W\ m^{-2}K)$
90	5.00	0.042	0.0144	377.71
90	5.00	0.047	0.0148	381.04
90	5.00	0.063	0.0162	388.53
90	5.00	0.078	0.0173	392.98
60	3.25	0.042	0.0179	512.48
60	3.25	0.047	0.0187	521.27
60	3.25	0.063	0.0212	543.53
60	3.25	0.078	0.0236	559.32
45	3.90	0.042	0.0163	482.91
45	3.90	0.047	0.0170	490.50
45	3.90	0.063	0.0189	509.25
45	3.90	0.078	0.0207	522.07
30	5.20	0.042	0.0141	433.96
30	5.20	0.047	0.0145	439.83
30	5.20	0.063	0.0158	453.73
30	5.20	0.078	0.0169	462.58

Assuming f_s= 0.011 and using (15), friction factor for this ribbed channel will be $\bar{f}$ = 0.0162.

This procedure can be applied for other rib blockage ratios and rib angles. Note that One may use C = 1.80 in (19) if 30°<α<90°, the results are shown in Table 2. Figure 12 shows temperature distribution at root of the blade for different rib angles.

Knowing that Nu_{smooth} = 79.60 and h_{smooth} = 224.2 W m^{-2} K and comparing these with values presented in Table 2, it is found that introducing the ribs in the channel regardless of the angle will increase heat transferred to the air, friction factor will always increase as well. Ribs mostly disturb only the near wall flow and consequently the pressure drop penalty by ribs is acceptable for blade cooling design, so introducing the ribs is always recommended.

Table 2 shows that maximum convection heat transfer coefficient, h and Nu for each α occurs when the rib blockage ratio is at maximum. It should be noted that when e/D_h increases friction factor also rises, therefore an enhancement of heat transfer is achieved with penalty of increase in the friction factor.

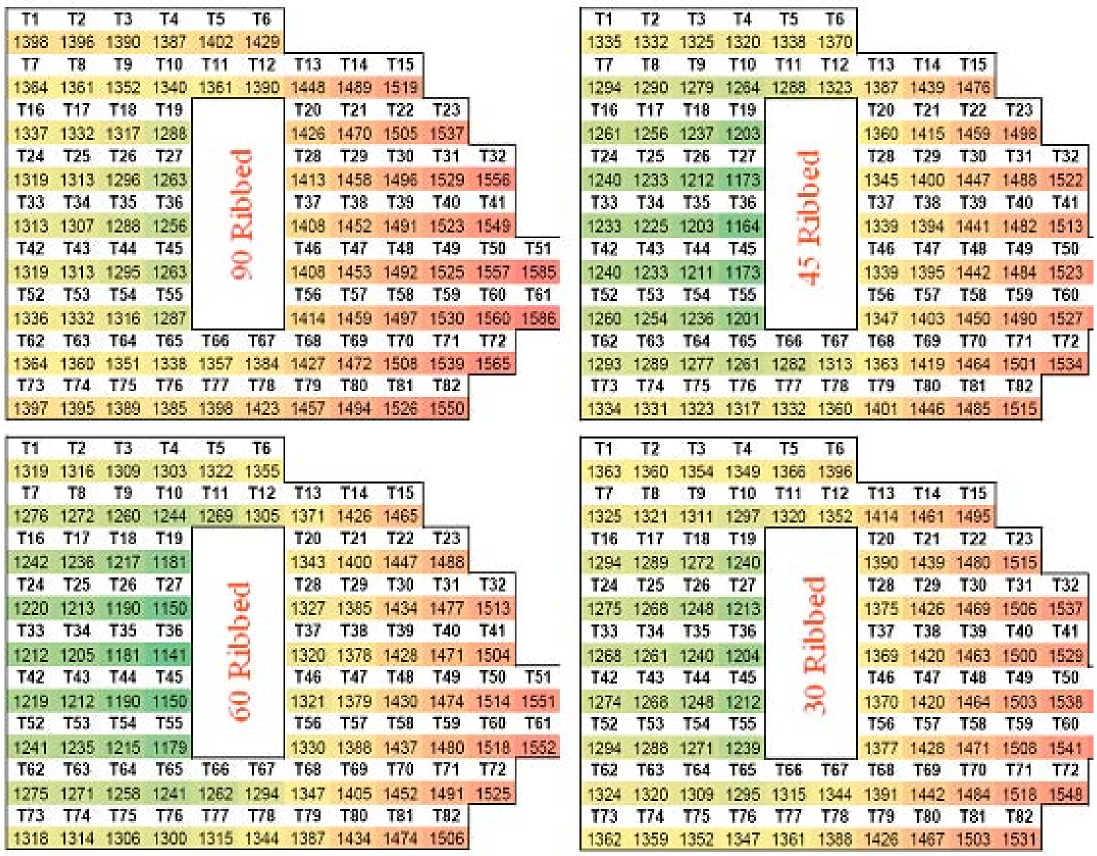

Fig. 12: Temperature (K) distribution in the cross section of GT blade surrounding ribbed cooling channel at root of the blade

Table 3: Comparison between different rib angles

α	Max temp. (K)	Min temp. (K)	q (W m^{-1})	ΔT air (K)
90	1586	1255	20693.3	428.6
60	1552	1140	26743.5	553.9
45	1559	1164	25482.5	527.7
30	1571	1204	23361.4	483.8
Smooth	1627	1407	13196.9	259.0

Comparing different rib angles, according to Table 2 maximum Nu value and h is achieved when 60° ribs are used in the channel with a rib blockage ratio of 0.078. Comparing with smooth channel (h_{smooth} = 224.22 W m^{-2}K) an enhancement of 149.45% is achieved with penalty of increase in the friction factor by 114.5%.

Table 3, compares maximum and minimum temperature, heat transfer per length as well as total increment in air temperature when leaving the channel.

CONCLUSIONS

Cooling system is very essential for Gas Turbines and has a direct effect on Gas Turbine efficiency. There are different cooling techniques available. Internal cooling is achieved by passing the compressed air through the internal channel provided in the blade and is enhanced by manufacturing the ribs inside the air passage.

- Among the rib angles, α of 90, 60, 45 and 30° and ribs blockage ratios, e/D_h ranging from 0.042 to 0.078, 60° ribbed channel with rib blockage ratio of 0.078 is recommended to be used for the gas turbine blade. An enhancement of 149.45% is achieved with penalty of increase in the friction factor by 114.5%
- Channels with 30° ribs are recommended to be used when pressure drop in the channel is important

- The effect of increasing heat transfer convection coefficient h in the air channel on cooling is far more effective than increasing thermal conductivity of the blade, i.e., the material
- Channels with 90° ribs do not have any advantages in terms of heat transfer enhancement comparing with other ribs even pressure drop in these channel is more than 30° case
- Transfer enhancement and pressure drop inside the passage. Ribs mostly disturb only the near wall flow and consequently the pressure drop penalty by ribs

Hence, using 90° ribs is not recommended at all when other ribs are available. Best ribs for heat transfer enhancement are those having angles and height to diameter ration of 60°, 0.078; 60°, 0.063; 45°, 0.078, respectively.

ACKNOWLEDGEMENT

The authors acknowledge Universiti Teknologi PETRONAS for supporting the project, technically and financially.

REFERENCES

Altorairi, M., 2003. Film cooling from cylindrical holes in transverse slots. M.S. Thesis, Louisiana State University.

Han, J.C., 1988. Heat transfer and friction characteristics in rectangular channels with Rib turbulators. J. Heat Transfer, 110: 321-328.

Han, J.C., S. Ou, J.S. Park and C.K. Lie, 1989. Augmented heat transfer in rectangular channels of narrow aspect ratios with rib turbulators. Int. J. Heat Mass Transfer, 32: 1619-1630.

Han, J.C. and S. Dutta, 1995. Internal convection heat transfer and cooling: An experimental approach. Von Karman Institute for Fluid Dynamics, Lecture Series on Heat Transfer and Cooling Gas Turbine, Belgium, May 8-12.

Han, J.C., S. Dutta and S.V. Ekkad, 2001. Gas Turbine Heat Transfer and Cooling Technology. Taylor and Francis, UK., pp: 289.

Han, J.C., 2004. Recent studies in turbine blade cooling. Int. J. Rotat. Mach., 10: 443-457.

Incropera, F., 2007. Introduction to Heat Transfer. 5th Edn., Wiley, New York.

Webb, R.L., E.R.G. Eckert and R.J. Goldstein, 1971. Heat transfer and friction in tubes with repeated-rib roughness. Int. J. Heat Mass Transfer, 14: 601-617.